

On the application of computer simulation techniques to anionic and cationic clays: A materials chemistry perspective

H. Chris Greenwell,^{†a} William Jones,^{*b} Peter V. Coveney^{*a} and Stephen Stackhouse^c

Received 16th May 2005, Accepted 8th September 2005

First published as an Advance Article on the web 14th October 2005

DOI: 10.1039/b506932g

The use of computational methods for the study of clay minerals has become an essential adjunct to experimental techniques for the analysis of these poorly ordered materials. Although information may be obtained through conventional methods of analysis regarding macroscopic properties of clay minerals, information about the spatial arrangement of molecules within the interlayers is hard to obtain without the aid of computer simulation. The interpretation of experimental data from techniques such as solid-state nuclear magnetic resonance or neutron diffraction studies is considerably assisted by the application of computer simulations. Using a series of case studies, we review the techniques, applications and insight gained from the use of molecular simulation applied to the study of clay systems (particularly for materials applications). The amount of information that can be gleaned from such simulations continues to grow, and is leading to ever larger-scale and hence more realistic classical and quantum mechanical studies which promise to reveal new and unexpected phenomena.

1. Introduction

Clay minerals are an example of a wider class of compounds known as layered materials, which may be defined as

^aCentre for Computational Science, Department of Chemistry, University College London, 20 Gordon Street, London, UK WC1H 0AJ. E-mail: p.v.coveney@ucl.ac.uk

^bDepartment of Chemistry, University of Cambridge, Lensfield Road, Cambridge, UK CB2 1EW. E-mail: wj10@cus.cam.ac.uk

^cDepartment of Earth Sciences, University College London, Gower Street, London, UK WC1E 6BT

[†] Current address: Centre for Applied Marine Science, Marine Science Laboratoires, School of Ocean Sciences, University of Wales Bangor, Menai Bridge, Anglesey, UK LL59 5AB.

“crystalline material wherein the atoms in the layers are cross-linked by chemical bonds, while the atoms of adjacent layers interact by physical forces”.¹ Both clay sheets and the interlayer space have widths in the nanometre range. The predominant naturally occurring cationic clay minerals have aluminosilicate sheets that carry a negative charge, which means that the interlayer guest species must be positively charged (cationic).² In anionic clays, the interlayer guest species carry a negative charge and the inorganic mixed metal hydroxide sheets are positively charged. Although the term layered double hydroxide (LDH) is more frequently applied, and is technically a more correct description, for clarity we shall refer in this article to these materials as anionic clays to



Chris Greenwell

Chris Greenwell studied for his BSc at University of Wales, Bangor, where he was awarded an entrance scholarship, the Evan Roberts prize, the Dr John Roberts Jones prize and the Peboe prize and medal, prior to undertaking his PhD (2003) in the Materials Chemistry Group, Cambridge under the supervision of Dr W. Jones. Research undertaken at Cambridge included the synthesis, characterisation and computer simulation of organic–inorganic hybrid materials.

Currently based at the Centre for Computational Science, University College London, his work addresses materials modelling, high performance computing and microscopy methods for analysing clays. In October 2005, he returns to the University of Wales, Bangor, to take up a position at the School of Ocean Sciences.



William (Bill) Jones

William (Bill) Jones was born in Mold, Flintshire and received his BSc and PhD from the University College of Wales, Aberystwyth. His early work, with Prof. Sir John Meurig Thomas and Prof. John O. Williams, was aimed at the use of low temperature transmission electron microscopy to analyse the nature of crystalline imperfections in organic solids. He moved to the University of Cambridge in 1978 and is a Fellow and College Lecturer in Natural Sciences at Sidney

Sussex College and Reader in Materials Chemistry in the University. His current interests include both clay chemistry and the materials chemistry of pharmaceutical solids. He is a co-Director of the Pfizer Institute for Pharmaceutical Materials Science.

emphasise their relationship with the more studied sheet aluminosilicate cationic clay materials. We shall refer to both types of material as “clays” when the discussion warrants it for the description of shared features, or as anionic and cationic clays to illustrate special features.

In recent times there has been a growing interest in anionic clays although, historically, attention has been focused almost exclusively on the cationic clay materials. Numerous reviews have appeared.^{3–5} Often these reviews emphasise interesting properties and the use of experimental techniques to determine or at least to infer the local structure of the clay sheet or intercalated material. However, clays are polycrystalline materials and precise experimental location of interlayer species is extremely difficult.

Only rarely can sufficiently large crystals for full structural determination by conventional single-crystal X-ray diffraction be obtained. Powder X-ray diffraction (PXRD) gives some indication of the bulk structure of the material (*e.g.*, the spacing between layers), but in general clay intercalates are characterised by the absence of significant long-range order. Interlayer arrangements (*e.g.*, guest orientation) may, however, sometimes be postulated from the interlayer spacing determined from PXRD measurements, but are frequently little more than educated guesses based solely on the assumed molecular dimensions of the guest.⁶ Whilst the distinction between mono-layer and bilayer arrangements, and the orientation of anisotropic interlayer guests, can often be inferred from the interlayer spacing determined by PXRD, the lateral arrangement of interlayer guest molecules, however, cannot be ascertained, and this is an area in which computer simulation can be usefully applied. Moreover, interlayer arrangements depend strongly on the interlayer water content of the clay as well as the nature of the intercalate, although this aspect is frequently overlooked.⁷ Indeed, the importance of water content has been ascertained through the use of molecular simulation.

Neutron diffraction can be used to ascertain the interlayer spacing in clays. It can also be used to determine the positions and self-diffusion of interlayer species that have been

isotopically labelled.^{8,9} Other techniques such as Fourier transform infra red (FTIR) spectroscopy, near edge X-ray adsorption fine structure (NEXAFS) analysis and Mössbauer spectroscopy have been used to characterise clays, but these give only limited information about the molecular structure and arrangement of guests within the interlayer region.¹⁰

Because of these limitations, interest in and the use of computational methods for studying these layered solids has increased in order that observed physical and chemical properties may be rationalised and even predicted. This review summarises the recent development of computational methods for studying cationic and anionic clays at the molecular level, that is to understand their materials chemistry. In Section 2 the structural features of anionic and cationic clays are briefly described. A summary of principal applications is given in Section 3. Section 4 gives a brief outline of computer simulation techniques in order to introduce the terminology necessary for the following sections. Subsequently, in Sections 5 and 6, the application of the different computational techniques for the study of anionic and cationic clays from a materials chemistry point of view is discussed through the use of several case studies. Finally, conclusions and the outlook for future simulation of clay-based materials are given in Section 7.

2. Structure of cationic and anionic clays

In this section the structure of cationic and anionic clays are outlined. Firstly, the two-dimensional sheet-like structure of the inorganic clay framework is described for both types of clays. This is followed by a description of the structure of the charge-balancing ions and associated water molecules within the interlayer region, and the types of forces within the clay system.

2.1 Structure of the clay sheets

Nearly all clay minerals are composed of continuous two-dimensional sheets stacked in a co-planar manner, but with a random in-plane phase. The various types of clays are



Peter Coveney

Peter Coveney holds a Chair in Physical Chemistry and is Director of the Centre for Computational Science (CCS) within the Department of Chemistry at University College London; he is also an Honorary Professor of Computer Science at UCL. He was the recipient of an HPC Challenge Award at Supercomputing 2003, and of an International Supercomputing Conference Award in 2004. Currently, Coveney is Chairman of the UK Collaborative Computational Projects (CCP) Steering Panel (www.ccp.ac.uk). Coveney has pioneered scientific grid computing including the use of computational steering to harness distributed grid infrastructure in order to solve challenging

problems in the physical and life sciences.



Stephen Stackhouse

Stephen Stackhouse received his MChem from the University of Manchester and PhD from Queen Mary, University of London. His doctoral research used first principles simulations to study the catalytic properties of the clay mineral montmorillonite and also the different mechanisms by which cis- and trans-vacant isomers of the structure dehydroxylate at high temperatures. He then moved to the department of Earth Sciences, at University College London, where his current work uses similar methods to determine the high temperature and pressure elastic properties of deep earth minerals.

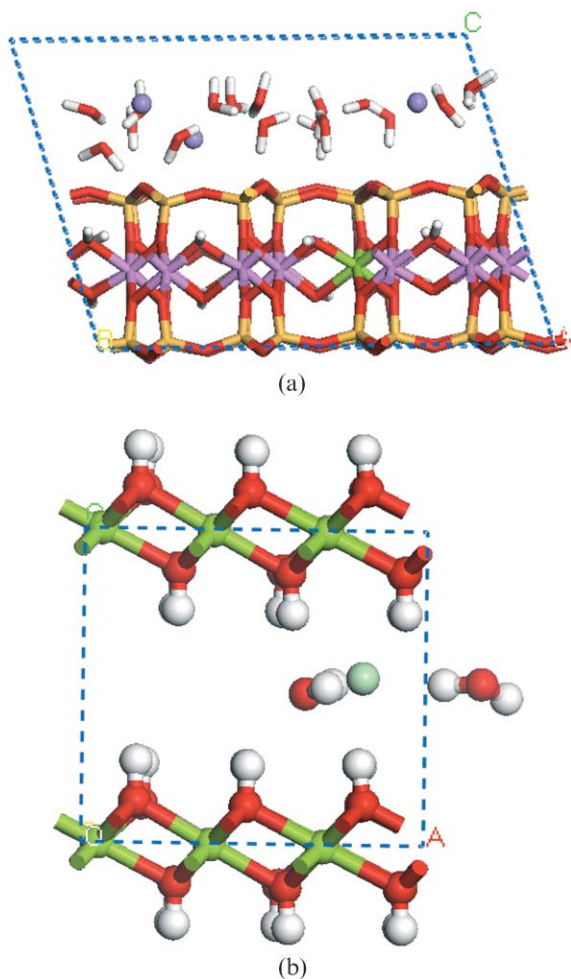


Fig. 1 Structure of (a) the cationic clay mineral sodium montmorillonite intercalated with organo-amine species showing the interlayer, tetrahedral layer and octahedral layer, and (b) a MgAl-LDH intercalated with chloride. The colour scheme is O = red, Si = orange, Cl = green, Na = brown, H = white, Mg = pink, Al = green. The unit cell is periodic in all directions.

distinguished by different atomic species in the sheets and the guest species present in the interlayer (*i.e.*, between the sheets). In fact, most clay minerals are based on one of a small number of common frameworks. Fig. 1 illustrates the structure of (a) the smectite cationic clay montmorillonite, and (b) the anionic clay composed of Mg and Al cations containing chloride as the charge-balancing ion. These are representative examples of the cationic and anionic clay families.

The cationic clays consist of two basic structural units: a tetrahedral sheet and an octahedral sheet. When the metal ions present in the octahedral sheet are divalent, such as magnesium, all octahedral sites are filled yielding a trioctahedral

clay. However, when trivalent cations such as aluminium are present, just two out of three sites are occupied and a dioctahedral clay is obtained. There are four common ways in which tetrahedral and octahedral sheets are found arranged together. These are listed in Table 1.

Further diversity in layer composition is generated by isomorphous substitution at tetrahedral and octahedral sites. The most common situation is that of partial substitution of silicon in the tetrahedral layer and aluminium or magnesium in the octahedral layer by atoms of similar size and coordination, but of different (usually lower) valency. The most common substituents for Si^{4+} are Al^{3+} and Fe^{3+} , while for Al^{3+} they are Fe^{3+} , Fe^{2+} and Mg^{2+} , though others are also found: for example, Mg^{2+} being replaced by Li^+ . Such a process gives rise to layers with a net negative charge. This is balanced by sorption of charge-balancing cations into the interlayer, and on surfaces and edges of the clay sheet.

Structurally, anionic clays may be considered as analogous to the magnesium hydroxide mineral brucite. Brucite consists of Mg^{2+} ions octahedrally coordinated by hydroxyl groups. The octahedra share edges in such a way that infinite sheets consisting of a single layer of octahedra are formed in the *ab* crystallographic plane. In the largest group of anionic clays some of the Mg^{2+} is substituted by a M^{3+} species, for example Al^{3+} , Fe^{3+} or Ga^{3+} . Other varieties of anionic clays exist where the M^{2+} species is for example Zn^{2+} or Ni^{2+} , giving rise to the family of compounds of general formula $\text{M}^{2+}_{1-x}\text{M}^{3+}_x(\text{OH})_2\text{A}^{x-}\cdot n\text{H}_2\text{O}$. A further family of materials may be derived based on the gibbsite ($\text{Al}(\text{OH})_3$) structure. Here the octahedral vacancies are filled by the inclusion of Li^+ cations, thereby generating a net positive charge. In each case the resulting structure consists of layers bearing a net positive charge, which is compensated by the introduction of anions in the interlayer region, as well as at the edges and surfaces of the anionic clay.

2.2 Arrangement of the charge-balancing species and water in the interlayer region

The interlayer contains the ions required to charge balance the inorganic clay sheets along with co-intercalated and adsorbed species (such as water). In naturally occurring clays the charge balancing ions tend to be small inorganic species, for example Na^+ or K^+ for cationic clays and CO_3^{2-} or Cl^- for anionic clays. However, these simple ions may be exchanged for (or synthetic clays prepared with) more complex species including alkyl ammonium species or carboxylic acids and polyoxometallates, in cationic clays and anionic clays respectively.

A common feature of both types of clay is the organisation of the interlayer region into hydrophilic and hydrophobic domains. This arises due to multiple factors, including the presence of water in the interlayer, the identity of the charge

Table 1 The classification of tetrahedral and octahedral sub-units into different clay types

Class	Example	Structure
1 : 1 Clay minerals	Kaolinite	Tetrahedral layer joined to one octahedral sheet.
2 : 1 Clay minerals	Pyrophyllite	Octahedral layer sandwiched between two tetrahedral layers.
2 : 1 : 1 Clay minerals	Chlorite	A 2 : 1 clay mineral structure between octahedral layers.
Pseudo-layer clay minerals	Sepiolite	2 : 1 layers arranged in chains. Not strictly layered materials.

balancing ion and the nature of the clay sheet. In the cationic clays hydration of the interlayer cations provides a driving force for the sorption of water into the interlayer of the clay minerals, where it associates with, and forms hydration shells around, the cations. The silicate surface of the tetrahedral layers of the cationic clays is relatively hydrophobic, resulting in intercalation of neutral organic molecules such as poly-ethers. In anionic clays, by comparison, the surfaces of the hydroxide sheets are very hydrophilic, though intercalated organic anions may result in a hydrophobic mid-plane region in the interlayer. The amphiphilic nature of the interlayer, particularly in organo-clays (those intercalated with organic material), leads to some self-assembly effects in the interlayer region.

A complex balance of repulsive and attractive Coulombic forces, hydrogen bonding, size of charge-balancing ion, hydration state (all enthalpic terms) and entropic contributions dictate how much material is contained in the interlayer and thus the interlayer separation, as well as intralayer local arrangement.

3. Applications of clay based materials

Owing to the useful properties of natural, modified and synthetic clays these materials have found diverse applications, some of which are briefly summarised here. The existence of a variable interlayer spacing is a common feature of many members of both the clay families of minerals. Cationic clays are natural Lewis acids, and upon washing with an acidic medium become mild Brønsted solid-acid catalysts.¹¹ Anionic clays exhibit the converse properties, becoming good solid-base heterogeneous mixed-metal oxide catalysts upon calcination.¹² The catalytic nature of the basic mixed-metal oxides is further increased upon re-hydration,^{13,14} or when intercalated with anionic bases such as *tert*-butoxide.¹⁵

These properties have resulted in the exploitation of clays as pharmaceutical delivery agents,¹⁶ for the protection and production of genetic sequences,^{17,18} environmental remediation catalysts,¹⁹ radiochemical storage media,²⁰ fillers in polymer composite materials,²¹ solid-acid or solid-base catalysts for many reactions,^{22,23} bio-mimetic catalysts,²⁴ drilling fluids,² paper coatings,²⁵ and sorbents.²⁶ To increase the thermal stability of the clay system for catalyst applications, the clay may be pillared to create a permanent three-dimensional architecture, somewhat similar to the industrially important zeolites, but with the important advantage that the pore size can be tailored.²⁷

4. Computer simulation techniques

The application and development of simulation techniques represent a vast area, with a diverse range of continually improving methods and techniques, and is dealt with thoroughly in various textbooks and monographs.²⁸ In order to familiarise the reader with some of the terminology necessary for the remainder of this article, we give a brief summary here. Techniques for the simulation of atomistic systems may, in general, be separated according to the accuracy with which they calculate inter-atomic interactions and the type of structural and statistical data that they provide.

4.1 Definition of the potential energy surface

The potential energy surface of a system describes the way in which the energy of the system changes with configuration, and plays an important role in simulation techniques. It is determined from the description of the interactions between individual particles. Broadly speaking, atomic interactions are determined at either the quantum or classical mechanical level; although semi-empirical methods, which lie somewhere in between the two levels of accuracy, also exist, but they will not be discussed here.

4.1.1 Quantum mechanics. Quantum mechanical simulations attempt to solve, to a good approximation, the fundamental equations of quantum mechanics, in order to model the interactions between the electrons and nuclei of a system of atoms. The advantage of quantum mechanical simulations is that they allow one to model electron dynamics in a process, such as bond-making/bond-breaking, as they have an explicit representation of electrons. In addition, the only input data necessary is the atomic number and initial configuration of the nuclei and the total number of electrons. The major disadvantage of the method is the massive associated computational cost—at present electronic structure calculations are limited to the study of hundreds of atoms, even when using large parallel computers.

4.1.2 Classical molecular mechanics. Simulation methods based on classical mechanics consider each atom as a single entity and the forces between them are modelled by potential functions based on classical physics. There is no description of interactions at the sub-atomic scale. In addition to initial atomic positions, one must also provide a set of suitable parameters for the interaction potential functions, known as a force-field. Parameters for force-fields are derived from experimental data and/or quantum mechanical calculations on a finite set of systems. Therefore the question arises as to how well a force-field is able to model the properties of systems dissimilar to those from which it was derived. Classical simulations are well suited to modelling of phenomena predominantly governed by non-bonded interactions. The use of simple inter-atomic potentials means that it is possible to handle up to millions of atoms and therefore model much larger and more “realistic” systems.

4.2 Structural and statistical data

Having calculated the potential energy surface there are various means by which it can be traversed and searched, of which we shall concern ourselves with three broad methods: geometry optimisation, molecular dynamics and Monte Carlo.

4.2.1 Geometry optimisation. The energy of a configuration of atoms may be minimized with respect to geometry (*energy minimization* or *geometry optimization*) by iteratively varying bond parameters, in a systematic way, to follow the curvature of a potential energy well until a minimum is reached. In theory, this should correspond to the observed molecular structure. The method, however, neglects thermal motion and

therefore only local minima on the potential energy surface may be searched.

4.2.2 Molecular dynamics (MD). By applying initial velocities to a configuration of atoms and solving Newton's equations of motion the potential energy surface may be traversed in a deterministic fashion and the temporal evolution of a system followed. This is known as molecular dynamics. In this technique thermal energy is included using a thermostat, which allows potential energy barriers to be overcome in a realistic manner. The main advantage of the method is that the dynamical evolution of a system, with time, may be followed, which allows comparison with additional experimental techniques such as NMR and quasi-elastic neutron scattering. It still remains a challenge, however, to follow the evolution of a system beyond the timescale of 1–10 ns, even when using classical mechanics simulations.

4.2.3 Monte Carlo (MC). Monte Carlo simulations involve searching the potential energy surface of a system by sampling many different configurations, generated by imposing random changes to a system according to a set of predefined rules. If the potential energy of a configuration is lower than the previous one then it is accepted. Those with higher energy are accepted with a Boltzmann-factor-weighted probability. Properties are calculated as the average of all accepted configurations.

Of the latter two methods, both have advantages depending upon the information desired from the simulation. MD simulation offers the advantage that the dynamical evolution of a system with time may be followed allowing comparison with time resolved experimental techniques such as NMR or FTIR. MC simulation, by contrast, is usually efficient for calculating thermodynamic averages for a system and can rapidly search a set of low energy configurations and find the global energy minimum in a shorter time than MD for a given set of computational resources, but allows no deterministic pathway to be followed across the potential energy surface. MC simulations can still produce averaged sets of low energy configurations that can be compared with quasi-elastic neutron scattering (QENS) or XRD data from experiment. In general, MC simulations are frequently carried out using rigid clay sheets and fixed interlayer spacing to allow the rapid calculation of the arrangement and loading of interlayer species, whereas MD simulations are carried out, often with flexible clay sheets and a variable interlayer spacing, to determine the effects that interlayer species have on the interlayer separation.

4.3 Statistical ensembles

The methods of traversing the potential energy surface described above may be carried out with various conditions imposed upon the ensemble of microstates that collectively define the system in a statistical mechanical sense. These conditions include, amongst others: constant number of atoms (N), pressure (P) and temperature (T) (the isobaric–isothermal NPT ensemble), and constant number of atoms, volume (V) and temperature (the canonical or NVT ensemble). The NPT ensemble most closely represents laboratory conditions in that conditions of constant external pressure and temperature are

maintained. In order to simulate processes such as swelling in a stochastic manner the system must be able to alter its volume, hence ruling out constant volume ensembles. However, in certain scenarios such as when the clay interlayer molecular loading and arrangement is being calculated for a known d -spacing from X-ray diffraction studies, constant volume ensembles, *e.g.*, NVT , may be employed and the model clay sheets kept locked at the experimentally observed separation. During energy minimisation an NVT ensemble is generally employed to remove unphysical interactions within the initial structures and then the unit cell parameters are systematically varied between minimisation cycles to attain a lowest energy configuration.

4.4 Modelling periodic systems

In order to represent the bulk structure of materials (greater than 10^{23} atoms) using relatively small models (generally less than 10^5 atoms), two approximations are often employed. These are (i) the use of super-cells, where the original unit-cell, usually derived from a crystal structure, is replicated several times and then redefined as one larger simulation cell and (ii) imposition of periodic boundary conditions on the simulation cell, where the super-cell is considered to be replicated infinitely in all three orthogonal space directions. Even though periodic boundary conditions would give representation of a bulk structure to small super-cells, or even unit cells, the super-cell employed must be large enough to remove artificial periodicity effects, where a molecule in one simulation cell is able to interact with its periodic replication in adjacent supercells. The use of periodic boundary conditions also has ramifications from the point of view of calculating long-range electrostatic interactions within the model since the charges associated with atoms and ions in the neighbouring cells have to be considered. In order to do this, long-range electrostatic interactions in periodic systems are generally calculated using the Ewald method, where the electrostatic interactions are summed over all interacting pairs of atoms to an infinite distance.²⁸ This is achieved by breaking the sum into two components, a direct sum which has a distance cutoff for interactions, and a reciprocal sum which uses Fourier transforms to calculate the infinite components and capture the interactions missed by the direct sum. In order to speed up the calculation of these long-range interactions, which are invariably computationally intensive, this method has evolved such that the reciprocal sum is mapped onto a mesh, allowing the use of fast Fourier transforms; such techniques are known as particle-mesh methods.²⁹ A further way of reducing computational demand is to calculate the long-range interactions at a lower frequency than the faster vibrational and bending bond interactions through the use of multi-timestepping integrators such as rRESPA.³⁰

4.5 Data analysis

Computer simulations provide large amounts of information on the electronic, atomic and molecular structure. Depending on the simulation method employed, further information can be extracted such as self-diffusion coefficients, radial distribution functions (RDF's), which reveal the coordination

environment of atoms, as well as mechanical properties such as elastic constants. Much of this computed data can be compared more or less directly with experimental measurements.

5. Examples of the application of molecular mechanics simulations to clays

Force-fields are often parameterised to fit a set of experimental data, or based upon detailed electronic structure calculations. However, there are relatively few force-fields able to reliably model well both the interlayer (often organic) species and the octahedral metal ion environments peculiar to the clay structure, particularly in the case of anionic clays. Force-fields that are specifically parameterised to model clay–organic interactions include those of Teppen *et al.*,³¹ and Cygan *et al.*³² The more generic Dreiding force-field has also been utilised, in a modified form, for modelling clay systems, especially LDHs.³³ It should be noted that all of the force-fields currently used for describing interactions within clay-based materials are based on the “pair-wise” interaction approximation, in which the problem of calculating interactions for a many-body system is reduced to the treatment of pair-wise interacting bodies. This approximation still yields data in good agreement with bulk properties of clay systems. Studies into the microstructure of water molecules and hydrated cations, however, using many-body force-fields have shown that to gain a more accurate understanding of the structure of water around strongly-polarising species, such as the cations present in the interlayer of hydrated cationic clays, many-body effects may need to be included within the simulations.^{34–36}

Force-field based simulations form the bulk of the literature on the modelling of clay systems. Kirkpatrick and co-workers have carried out much work on LDHs from a geochemical perspective,^{37–41} in which experimental NMR and FTIR data have been interpreted through the associated use of molecular dynamics (MD) simulations using the ClayFF force-field of Cygan *et al.*³² Similarly, Skipper, Coveney and others have investigated the structure of interlayer water and cations within smectite clays using force-field based models.^{42–44} Yamagishi and co-workers have used force-field based Monte Carlo methods to rationalise the binding of metal complexes in the interlayer of cationic clays.^{45–47} Force-field based molecular dynamics simulations have been used to determine the elastic properties of clay sheets, an important property for the prediction of bulk materials properties.^{48,49}

5.1. Simulating swelling properties of clays

One of the commonly encountered properties of most clay minerals is their ability to swell or contract, depending on the amount of water, or other solvent, present. This has important implications for many applications of clay minerals. From a chemical point of view the variable swelling gives clay minerals increased potential for intercalating bulkier molecules and allows for a variable interlayer spacing for increased substrate specificity in catalysis (see Section 6.1, for example). Understanding and controlling the swelling of clays has important implications for the fine chemical industry, the

construction industry and also in drilling for oil and water. Owing to the greater abundance of cationic than anionic clays, cationic clays have been subject to many more studies, both experimental and computational, than anionic clays.

5.1.1 Controlling the interlayer separation of anionic clays: swelling of terephthalate LDHs. One of the earliest examples of simulation of anionic clays relates to terephthalate exchanged materials. A potential problem in the use of anionic clays as industrial catalysts is the thermal instability arising due to the two-dimensional nature of the sheets, resulting in structural collapse at elevated temperatures. At very high temperatures the sheets themselves decompose. To prevent the layers collapsing it became attractive to “pillar” the anionic clay with immobile inorganic pillars, turning the two-dimensional clay into a tailored three-dimensional porous solid.^{1,27} However, the incorporation of the pillaring material into the interlayer was not facile, due to the unfavourable low charge to mass ratio of the compounds used being unable to compete with the existing anions in the interlayer. This was subsequently resolved through pre-expanding the layers by using an intermediate “expansion” species, such as terephthalic acid, because of the relatively large size of the anions and the pre-expansion involved during their uptake.⁵⁰ Powder XRD analysis showed that terephthalic acid adopted a variety of interlayer spacings, depending upon anionic clay composition.^{7,51}

The first simulations of anionic clays were carried out by King and Jones, who used a set of simple potentials to minimize the energy of a set of small anhydrous simulation cells, including one with terephthalate present.⁵² The authors achieved relatively poor agreement with experiment and attributed this to the absence of water in their simulation, illustrating the important effect that hydration state has in maintaining interlayer spacings and arrangements. More reliable studies were later made by Aicken *et al.* who performed simple minimization studies of terephthalate-anionic clays,⁵³ a study which was further expanded upon by Newman *et al.*, who used molecular dynamics simulations to model Mg₃Al- and Mg₂Al-anionic clays containing interlayer terephthalate anions and varying numbers of water molecules in order to rationalize the experimentally observed interlayer separations in terms of the anion arrangements.⁷

Results from the simulations were compared with powder X-ray diffraction and thermogravimetric measurements performed on synthetic Mg₃Al- (a Mg and Al anionic clay where Mg : Al = 3 : 1) and Mg₂Al-anionic clays containing terephthalate.⁷ Different water contents were obtained by hydrating, or dehydrating, the synthetic anionic clay to different extents. Fig. 2 shows schematically the results from these studies. In summary, the experiments revealed that an interlayer spacing of approximately 14.0 Å is favoured by high layer charge and high interlayer water content. This spacing is suggestive of the terephthalate anion being in a predominantly perpendicular orientation with respect to the anionic clay sheet (shown in Fig. 2a). For low layer charge and water content an interlayer spacing of approximately 8.4 Å was observed, which correlates with the terephthalate anion lying parallel to the anionic clay sheets (Fig. 2b). During cycles of dehydration–rehydration, the PXRD data suggested that the 14.0 Å and

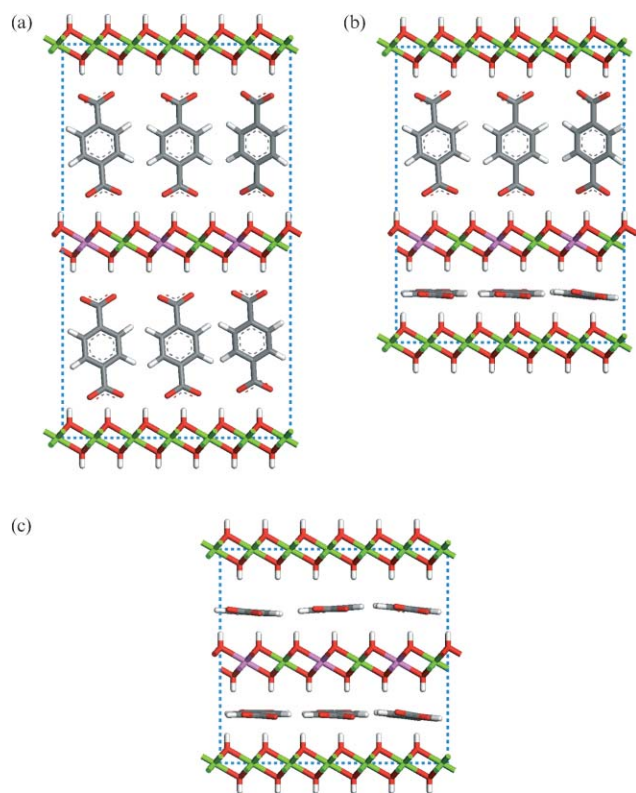


Fig. 2 Schematic to show the possible experimentally observed interlayer arrangements in terephthalate intercalated LDHs with (a) showing the expanded arrangement where the anions are perpendicular to the LDH sheets, (b) the interstratified arrangement, and (c) the collapsed structure where the anions lie parallel to the LDH sheets. The colour scheme is the same as used in Fig. 1.

8.4 Å interlayers coexist in varying proportions depending on the layer charge and water content and, in certain cases, 22.4 Å interstratified phases consisting of a regular alternation of the component interlayer was identified (Fig. 2c).

A computer simulated swelling curve was obtained for the model Mg_3Al -terephthalate anionic clay.⁷ The interlayer spacing increased gradually from approximately 8.5 Å for the model without interlayer water to approximately 15 Å for the model containing 30% by weight of water. The gradual expansion of the interlayer with increasing water content was accompanied by a gradual change in the orientation of the terephthalate anions from horizontal to vertical, with respect to the hydroxide layers. A simulated swelling curve was also obtained for the model Mg_2Al -terephthalate anionic clays. The interlayer spacing was found to increase gradually with increasing water content before levelling off at approximately 14.0 Å for a water content of approximately 20 mass%. This is in good agreement with the experimentally determined water content for the synthetic anionic clay with similar interlayer spacing. In the simulated systems, fewer water molecules are required to ensure a vertical orientation of the terephthalate anions in the Mg_2Al -anionic clay compared to the Mg_3Al -anionic clay, presumably due to the higher layer charge and increased interlayer anion packing density for $\text{Mg} : \text{Al} = 2$.

The simulations performed to obtain the swelling curves did not reproduce the experimentally observed interstratified

arrangement for the synthetic terephthalate anionic clay with intermediate water contents.⁷ The observation of the interstratified phase suggests an ordered alternating sequence of relatively hydrated and dehydrated interlayers with the terephthalate anions in either a vertical or horizontal orientation, respectively. The use of periodic boundary conditions, a constant number of atoms, and imposed symmetry (*i.e.*, an equal number of water molecules per interlayer) of the simulations, however, makes it impossible to predict such situations as water molecules may not leave the interlayer regions. Additional molecular dynamics simulations (NPT) were performed, therefore, on the Mg_2Al -anionic clay model with an unequal distribution of the water molecules between the two interlayers of the simulation cell. The results from these simulations suggest that the interstratified phase may consist of alternating relatively dehydrated and hydrated interlayers.⁷

The properties of the interlayer water in the Mg_3Al -terephthalate with 64 water molecules and the Mg_2Al -terephthalate LDHs with 44 water molecules were further investigated using data extracted from an additional NPT molecular dynamics simulation, to improve the statistics. In both these models, the terephthalate anions adopted a vertical orientation with respect to the hydroxide layers and the simulated interlayer spacings were in good agreement with experiment. The radial distribution function (RDF), which gives the probability of finding a pair of atoms separated by a given distance relative to the probability expected for a completely random distribution at the same density, has been calculated for water oxygen atoms to investigate the nature of the simulated interlayer water. The calculated water O–O RDF for the models exhibited the same principal features as the simulated RDF obtained for bulk water (using the TIP3P force-field parameterisation) by Boek *et al.*⁵⁴ A well-defined peak at 2.9 Å indicated a relatively high degree of structural ordering of the water molecules within the first coordination shell, probably within a single surface monolayer located adjacent to the clay surfaces. A second peak at 5.7 Å, poorly defined compared with the first, suggested that a second hydration shell also exists.³³

The water self-diffusion coefficients, D , calculated for both models were of the same order of magnitude as experimental data obtained using quasi-elastic neutron scattering ($D = 2.47 \times 10^{-7} \text{ cm}^2 \text{ s}^{-1}$ for a synthetic Mg_2Al -terephthalate anionic clay at 50 °C).⁹ As would be expected for water constrained between the hydroxide layers of an anionic clay, the simulated water self-diffusion coefficients were significantly lower than values obtained from simulations of bulk water ($1.88 \times 10^{-5} \text{ cm}^2 \text{ s}^{-1}$ at 300 K, using the Dreiding force field with TIP3P water parameters)⁵⁴ or experimental values obtained for bulk water ($2.3 \times 10^{-5} \text{ cm}^2 \text{ s}^{-1}$ at 298 K).⁵⁵

The relative size of D calculated for the two models suggested that the interlayer water molecules were more mobile in the Mg_3Al model compared with the Mg_2Al model. This observation may be understood in terms of the relative charge densities of the layers—the higher the charge density, the more tightly bound the polar water molecules to the clay sheet—as well as the lower amount of interlayer space occupied by terephthalate in the Mg_3Al system.

Williams *et al.*, using the same techniques, studied the effect of methanol *versus* water on the swelling properties of Mg₂Al-terephthalate anionic clays.⁵⁶ The results showed that the swelling curve for water reached a plateau at approximately the experimental interlayer spacing (value of *circa* 14.0 Å, with the water content at 20 wt%). The water self-diffusion coefficient was calculated to be $5.90 \times 10^{-7} \text{ cm}^2 \text{ s}^{-1}$, which was also in good agreement with experiment.⁹ At higher water content a sharp increase was observed in the simulated swelling curve. At these higher water contents the terephthalate anions in the simulation cell were observed to become detached from one LDH layer face with the interposition of water molecules between the anion and the LDH layer. With methanol as the solvent no plateau region in the swelling curve was calculated (no experimental studies of terephthalate-anionic clays in methanol have been carried out), suggesting that these systems may not have meta-stable interlayer spacings and therefore might exfoliate. When a clay exfoliates the clay sheets become separated and dispersed resulting in very little stacking, a state hard to achieve in anionic clays except under certain special conditions.⁵⁷ The use of exfoliated clays in the preparation of clay-polymer nanocomposites is currently an area receiving much attention, *vide infra*.

5.1.2. Developing drilling fluids to inhibit clay swelling in the oilfield industry: hydration of smectite clays. During well-bore construction in the petrochemical industry organic additives are added to water-based drilling fluids in order to inhibit the swelling of clay mineral formations that might result in damage to both the well and the drilling equipment. These additives are designed to be sorbed into the interlayer of clay minerals and there inhibit swelling to preserve well-bore integrity.

The mechanism by which organic additives inhibit the swelling of clay minerals was investigated by Bains *et al.*,⁵⁸ who performed Monte Carlo, energy minimisation and molecular dynamics simulations to model the sorption of polyethers into the interlayer of the clay mineral montmorillonite. These simulations showed that the preferential sorption of the organic molecules into the interlayer, rather than water, is driven by entropic factors: a single long chain polyether can displace a large number of small water molecules within the clay interlayer, each of whose translational entropy is greatly increased when removed from the interlayer.

Inspection of the resultant interlayer arrangements indicated that good swelling inhibitors are of medium to high molecular weight and possess well-defined hydrophobic regions separated by hydrophilic regions. It is thought that the hydrophobic regions seal against the ingress of water, while the hydrophilic regions aid the binding of the inorganic cations (attached to the clay surface) to the interlayer, preventing their hydration and therefore swelling.

5.2. Understanding photochemistry in constrained media: predicting reactivity in cinnamate LDHs

The interlayer spacing in organo-clay materials is invariably within the nanometre range. As such, any intercalated material is constrained within a nanoscale environment. This

environment can be used to arrange reactant molecules in specific proximities and orientations, so as to enable otherwise unfavourable reactions to occur, or to selectively favour certain products.⁵⁹ Certain reactions between organic guests within anionic clays have been found to be strongly dependent upon the Mg/Al ratio of the clay host. Since the effect of varying the Mg/Al ratio is reflected in the interlayer arrangement of the reacting organic species, simulation can often provide insight into pre-reaction conditions that may not be accessible by any other method.

Valim *et al.*, Takagi *et al.*, and Shichi *et al.* have experimentally examined the photochemical dimerisation of cinnamate anions within the interlayer of MgAl anionic clay systems.^{60–62} The products of these reactions were found to depend on the charge on the clay sheet, and hence the amount and distribution of reactive species in the interlayer, different stereo-chemical dimers being favoured at different Mg/Al ratios, suggesting that the constraining nature of the anionic clay host imposed stereo- and regio-selectivity upon the reaction.

Though classical, empirical, force-field based simulations cannot be used to simulate chemical reactivity, there are methods by which these techniques can be used to give insight into the probable outcome of chemical reactions. Classical MD simulations have been carried out to model the interlayer arrangement of these systems at various Mg/Al ratios and hydration states, and a “retrosynthesis” approach used to infer the outcome of reactions within the anionic clay interlayer.⁶³ Dimer precursors, reflecting the pre-reaction cinnamate monomer positions, were generated based on optimised models of the possible dimer molecule products (Fig. 3). Independently, close contacts at distances favourable for photodimerization between the reacting double bonds on the cinnamate molecules were monitored in the equilibrated NPT MD simulations at a temperature of 298 K. Where close contacts occurred the pair of adjacent cinnamate molecules involved, from the MD simulations, was compared to the various dimer precursor pairs generated previously. The precursor pair most similar to the arrangement of the adjacent cinnamate molecules, and hence the dimer from which they were derived, was deemed to be the most probable outcome of any photochemical reaction that might ensue.

Within the assumptions made in the simulations, reasonable agreement was found with the experimental results. Fig. 4 illustrates the effect of both Mg/Al ratio and hydration state on the interlayer arrangement of cinnamate intercalated MgAl-anionic clays. In the experimental work of Shichi *et al.* it was observed that as the Mg/Al ratio increased, *i.e.*, the charge on the clay sheet decreased, the ratio of *syn*-HH to *anti*-HH dimer decreased and the proportion of *cis*-isomer in the product mixture increased. The absence of any significant *syn*-HT dimer formation at low Mg/Al ratio was taken to confirm that steric control was operating and that a bilayer arrangement of anions perpendicular to the sheets must result in olefin-olefin distances too great for dimer formation.⁶² The computational results show some agreement with the experimental data, the dominant species predicted at low Mg/Al being the *syn*-HH dimer. For increased Mg/Al ratios and water content the *anti*-HH dimer is observed to be the likely product,

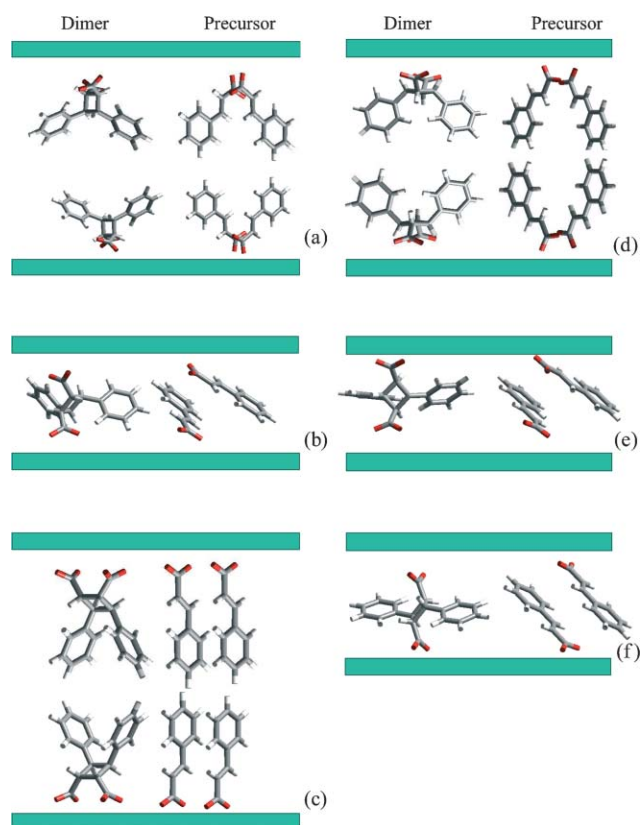


Fig. 3 Schematic to show the various possible dimers and the dimer precursors: (a) *anti*-HH (bilayer), (b) *anti*-HH (monolayer), (c) *syn*-HH (bilayer), (d) *anti*-HT (bilayer), (e) *anti*-HT (monolayer), and (f) *syn*-HT (monolayer). The green rectangles represent the LDH layers. In each case the organic molecules are oriented with the carboxylate group adjacent to the hydrophilic LDH sheet, and the hydrophobic aromatic ring in the mid-plane of the interlayer region.

whilst at the highest Mg/Al ratio simulated the dominant outcome would appear to be the *cis*-isomer. The *syn*-HT dimer is not predicted to form at low Mg/Al ratios: under moderate hydration conditions the lack of a fully interdigitated bilayer arrangement precludes its formation by cinnamate molecules attached to opposite hydroxyl layer faces.⁶³

Shichi *et al.* rationalized an observed transition from *syn*-HH to *anti*-HH dimer formation with increasing inter-Al³⁺ distance (*i.e.*, increasing Mg/Al ratio) favouring the formation of the *anti*-HH dimer, which requires a longer inter-carboxylic distance when compared to the *syn*-HH dimer.⁶² This simple intuitive model, however, fails to account for both the absence of the *anti*-HT dimer and the formation of HH dimers in the system with Mg/Al = 6, since in this case the average distance between Al³⁺ centres will be 8.2 Å, far exceeding the distance of 4–5 Å required for [2 + 2] cycloaddition to occur.⁶¹

The absence of *syn*-HT dimers in LDHs with Mg/Al = 6 in the experimental work of Shichi *et al.* suggests that the experimental water content of the LDH is in excess of 20 wt% and that the cinnamate anions most likely adopt an interdigitated bilayer arrangement favoured by the greater hydration state.⁶² The simulation work does not, however, account for the observed formation of *syn*-HH dimers and *anti*-HH dimers at Mg/Al = 6. Possible explanations include

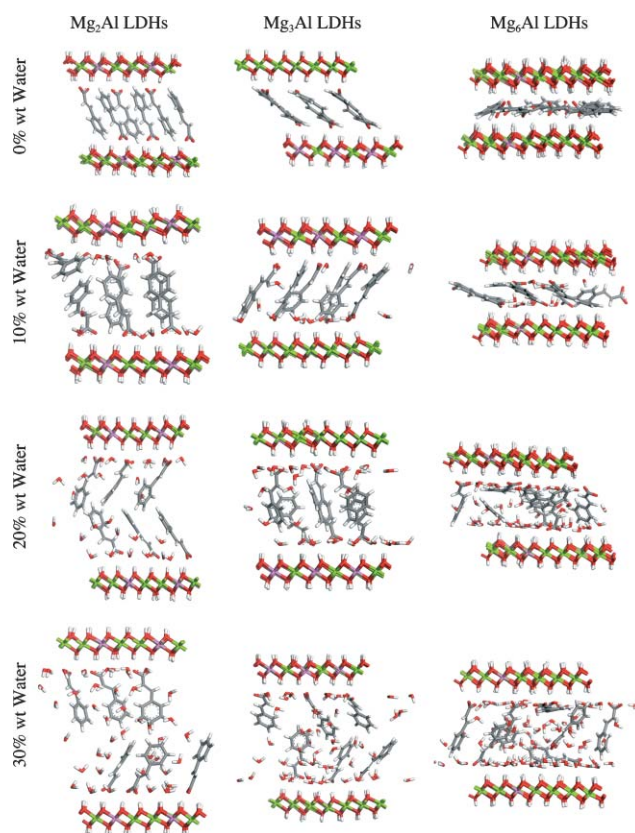


Fig. 4 Snapshots taken after 40 ps of MD simulation to show the effect of hydration state and Mg/Al ratio on the interlayer arrangement of MgAl cinnamate-LDHs. The colour scheme is the same as used for Fig. 1.

the following: (i) the cinnamate anions exhibit clustering to a greater degree than observed in the modelled structures; (ii) Al³⁺ may be disordered at long ranges, but exhibits short-range order corresponding to domains of a higher Mg/Al ratio in the hydroxyl sheets; (iii) that these products ensue from interlayer arrangements dictated by the lower than theoretically expected local cinnamate density in the experimental interlayer loadings, resulting from incomplete anion exchange and hence uptake of cinnamate by the initially chloride-containing anionic clay.⁶³

In general it was found that the interlayer arrangement was more dynamic than anticipated and though the cinnamate carboxylate group was invariably oriented towards the MgAl layer the position of the remainder of the anion was quite fluxional. This resulted in pairs of molecules sometimes matching, over the simulation period, the criteria for photo-dimerization and not at other times. For studying chemical reactivity quantum mechanics is usually required (see later in Section 6), but the study of excited states in periodic models using density functional based methods is not routine, and highly non-trivial (See Section 7 for emergent techniques in this area).

5.3. Interlayer structure in clay–polymer nanocomposites

Over the last decade there has been interest in the use of composites consisting of clay platelets embedded within a

polymer matrix. Initially cationic clays were investigated,²¹ but recently there has also been increasing interest in the use of LDHs for related and distinct applications.⁶⁴ These materials have been found to have similar properties to conventional composites, but for substantially lower amounts of filler material. Furthermore, the resulting composites can be easily processed to form films with improved barrier properties to gases, and materials with improved fire-retarding ability.²¹ Owing to the nanoscale of both the clay platelets and the interlayer spacing between the clay sheets, these compounds became known as nanocomposites.⁶⁵ In clay-polymer nanocomposites containing Li^+ cations the arrangement of the polymer parallel to the clay-sheets gives improved ion conduction for potential applications as battery materials.⁶⁶ The simulation of clay-polymer systems has received some attention from materials simulation groups, for example Fermeiglia and co-workers have investigated the binding energy of various polymers with clay platelets using molecular dynamics methods.⁶⁷⁻⁶⁹

A problem in the synthesis of clay-polymer nanocomposites using cationic clays arises due to the inorganic cations, as their associated hydration shells prevent the intercalation of polymer into the interlayer region. To circumvent this, it is attractive to exchange the inorganic cations with organic cations, normally tertiary ammonium compounds, thereby rendering the interlayer region organophilic and greatly expanding the interlayer separation to facilitate incorporation of the polymeric material.⁷⁰

However, in instances where low molecular weight primary amines are utilised, the only interlayer spacing observed corresponds to a monolayer arrangement of organic material while FTIR analysis indicated that increased hydrogen bonding occurs within the interlayer region relative to an analogous primary ammonium intercalated clay, similar to systems where a mixture of ammonium and amine species are co-intercalated.⁷¹⁻⁷³

Simulation studies using large-scale MD methods (see Section 4.4) showed that at the experimental organic loadings a monolayer of the poly(propylene oxide) diamine monomer forms.⁷³ If the amine groups are protonated, *i.e.*, to form ammonium groups, a conformational change in the monomers occurs, whereby the ammonium cation strongly coordinates with the surface oxygen atoms of the tetrahedral clay sheet and a slight increase in basal spacing occurs. The similarity between interactions of the ammonium organic cations and Na^+ inorganic cations with the clay sheet is shown in Fig. 5. In models in which only some of the amine groups are protonated to form the ammonium species, both intra- and inter-molecular H-bonds form between amine N atoms and ammonium H atoms, accounting for the increased H-bonding observed in the FTIR spectra and indicating that a mixture of ammonium and amine species are present in the interlayer of the experimental system, as suggested by the experimental evidence.

In some instances where a high clay fraction is required, such as the stabilization of oilfield well-bores (Section 5.1.2),⁷⁴ it is desirable to produce clay-polymer nanocomposites through the *in situ* polymerization of small monomer molecules within the clay galleries.⁷⁵ In order to rationalize

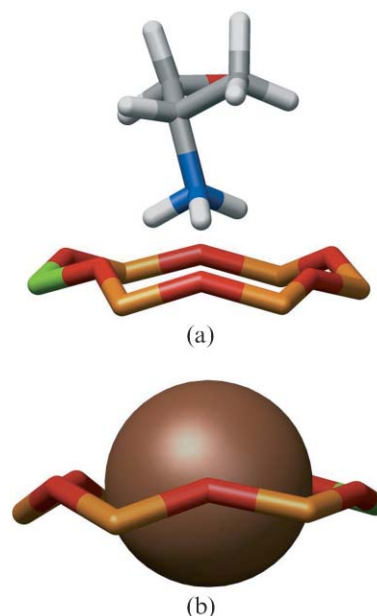


Fig. 5 Snapshots after 1 ns of MD simulation of 7160 atom models showing (a) the interlayer arrangement of ammonium cations and adjacent clay sheet atoms (other atoms omitted for clarity). The ammonium cation is arranged to maximise H-bond and electrostatic interactions. When compared to the Na^+ cation, (b) the ammonium cation is unable to sit closer to the cavities in the tetrahedral layer of the clay sheet due to steric restrictions and strong H-bond interactions with surface O atoms.

reactivity in these systems it is necessary to understand the interlayer arrangement of the reactive centres, where polymerization or cross-linking occurs. Force-field based simulations have been used to examine issues such as how the nature of the monomer backbone, monomer head-group and identity of interlayer cations affect the arrangement of intercalated monomers.^{72,76} As in the work on terephthalate anionic clay systems (Section 5.1.1), these studies were carried out in tandem with experiments to ascertain monomer and water loadings in the simulated systems.

For simulated poly(ethylene glycol) nanocomposites no evidence was found for hydrogen-bond interactions between the protons of the PEG alcohol groups and the tetrahedral oxygen atoms of the clay surface.⁷⁶ It seems therefore that, in the presence of water and cations, poly(ethylene glycol) is unlikely to form strong H-bonds to the clay surface. When functionalised with terminal acrylate or alcohol groups, the poly(ethylene oxide) chains tend to orientate with the O atoms towards the mid-plane for the Na^+ and Li^+ clays, away from the cations which reside at the clay sheet face. This arrangement, which results in organic monomer C atoms adjacent to the organophilic silica surface, has been reported previously by others.⁶⁹

The choice of monomer was also found to affect the cation distribution across the composite interlayer. In the poly(ethylene glycol) composites hydroxyl groups retained some of the cations and associated hydrations shells within the mid-plane of the interlayer region. The magnitude of this effect was dependent upon the cation present in the simulated clay

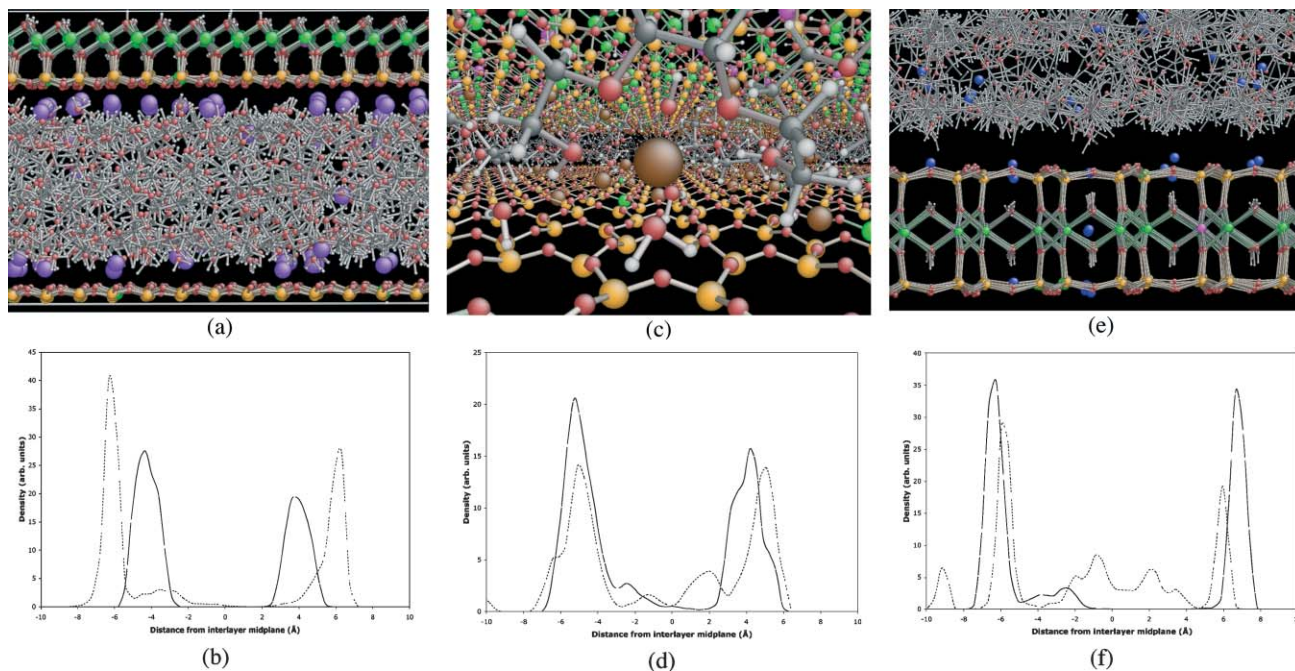


Fig. 6 Snapshots taken after 1 ns of MD simulation showing the interlayer arrangement in poly(ethylene glycol) montmorillonite composites where (a) K^+ is the exchangeable cation, (c) where Na^+ is the exchangeable cation, (e) Na^+ is the exchangeable cation, and the corresponding time averaged 1-dimensional atom density plot across the interlayer region for the different cations, (b) K^+ , (d) Na^+ , (e) Li^+ where: dashed line = poly(ethylene glycol) and solid line = poly(ethylene oxide) diacrylate for comparison. Organic material and water content are based on experimental measurements.

composite, with the high surface charge density Li^+ more susceptible than Na^+ , while the majority of the K^+ ions migrated to the face of the clay sheet. Snapshots of these systems after 1 ns of MD simulation and the derived 1-dimensional atom density plots, which show the time averaged atom density for the cations relative to the mid-plane of the interlayer region, are shown in Fig. 6. Since the cations are retained in the interlayer region they are also more closely associated with the monomer backbone O atoms. Therefore, in the radial distribution functions, the order of interaction for both the poly(ethylene glycol) hydroxyl O atoms and the backbone O atoms with the cations is: $Li^+ > Na^+ > K^+$.⁷⁶

Conversely, the poly(ethylene oxide) diacrylate monomers, having no hydroxyl groups, do not retain the cations in the interlayer region, resulting in the vast majority of the Li^+ and Na^+ cations migrating into vacancies on the tetrahedral layer of the clay sheet, with the K^+ cations migrating to the face of the clay sheets. This prevents the Li^+ cations, effectively charge-shielded by the O atoms at the clay surface and associated water molecules, from interacting with the monomer oxygen atoms. Comparison of the interaction between the different cations and the poly(ethylene oxide) diacrylate backbone and endgroup O atoms confirms this, showing preferential interaction with the low surface charge density cations, *i.e.*, in the order: $K^+ > Na^+ > Li^+$.⁷⁶

5.4 Large-scale molecular dynamics and mesoscale modelling

Recent advances in computer hardware and algorithms have allowed computer simulations to be efficiently domain

decomposed and run efficiently in parallel on multiple processors of large supercomputers. There are now several scalable molecular dynamics codes available that can be used for efficient high performance parallel computing, the scalability of many of which have recently been reviewed by Hein *et al.*⁷⁷ Such codes are essential for including macromolecules or polymers within clay simulations and also enable us to probe the hitherto often-overlooked existence of finite-size effects in smaller models. Katti *et al.* have recently used the NAMD code, commonly employed for modelling large-scale biological molecules, to examine the response of pyrophyllite clays to applied stress.⁷⁸ The large-scale atomic/molecular massively parallel simulator (LAMMPS) code is particularly suitable for the large-scale simulation of materials systems such as clays.⁷⁹ Coveney and co-workers have exploited the capabilities of LAMMPS to simulate clay-polymer nanocomposite systems up to and beyond 1 million atoms.^{73,80} The group has observed that, for simulation cell sizes in excess of 250 000 atoms, undulations occur in the clay sheets (Fig. 7), reminiscent of those reported elsewhere for biological bilayers,⁸¹ and by Sato *et al.* for single clay layers under applied stress,⁸² which should allow mechanical properties such as elastic constants to be extracted from the simulation data in future studies. These may allow comparison with, and prediction of, experimental data such as ultrasonic measurements. At these length scales the simulation supercells are *circa* $50 \times 50 \times 3$ nm, approaching the dimensions of clay sheets and tactoids typically observed in electron micrographs. As the number of atoms simulated continues to increase it is now becoming

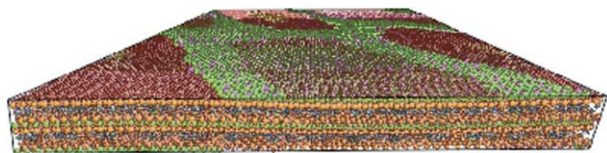


Fig. 7 Snapshot of 350 840 atom supercell ($14 \times 14 \times 2$ replication of unitcell) of poly(propylene oxide) diammonium Na^+ -montmorillonite after 0.5 ns of MD simulation showing a perspective view of the rectilinear supercell, the clay sheets exhibiting gentle undulations. The colour scheme is: C gray, H white, O red, N blue, Si orange, Al green, Mg magenta, and Na brown. Periodic boundary conditions are imposed in all 3 orthogonal space directions.

possible to consider simulating “real size” clay sheets without using periodic boundary conditions.

To access even larger simulation length and time scales, where the clay platelets themselves are embedded in a polymer matrix and thus are not constrained by periodic boundary conditions, it becomes necessary to employ a further type of dynamic simulation, meso-scale modelling, which is similar to molecular dynamics but at a coarse-grained level. The clay and the organic molecules in these simulations are all simply represented by chains of spheres (beads), with the bonded interactions typically represented by simple harmonic functions. Using such techniques the diffusion of functionalized polymers into clay systems has been studied by Sinsawat *et al.*⁸³ The authors modelled tactoids of clay sheets in a polymer melt and found that polymers with headgroups that strongly interacted with the clay sheet do not tend to intercalate fully, the headgroups remaining at the edge of the clay interlayer while the backbone of the polymer intercalates.

6. Electronic structure investigation of clay systems for materials applications

In order to model any chemistry within condensed matter systems, which involves the breaking or forming of bonds, it is necessary to perform calculations on the electronic structure of the system to be studied, *i.e.*, using quantum mechanics.²⁸ There have been several studies of cationic clay systems using these methods, but very little work has been carried out on anionic clays.

In early work, *ab initio* electronic structure calculations were carried out using small fragments, usually referred to as clusters of atoms, to represent the clay in order to develop parameters for molecular mechanics force-fields,^{84,85} or to obtain detailed structural information about the clay sheets.⁸⁶ More realistic simulations followed, in which the clay sheet was represented as an infinite replication of a small periodically repeated unit cell and a computational faster, albeit more approximate, plane wave density functional theory (DFT) approach was employed, allowing larger numbers of atoms to be treated. In addition to the applications discussed here, the use of electronic structure simulations using these periodic models has found uses in gaining insight into clay sheet structure,^{87–89} thermal behaviour of clays,^{90,91} reactivity of clays for environmental remediation,^{87,92,93} interlayer water

structure and dynamics,^{89,94,95} and to obtain parameters from which to develop suitable clay–organic force-fields.³¹

6.1. Modelling catalytic cycles in solid base catalysts: *t*-butoxide organo-LDHs

Plane-wave based DFT simulations have been carried out to investigate possible catalytic pathways in $\text{MgAl-}t\text{-tert}$ -butoxide LDHs.⁹⁶ These materials have been reported in the literature for their “super-basic” properties, as they catalyse a range of reactions.^{97–100} Plausible reaction mechanisms have been suggested based upon the products of one such reaction, transesterification, and this has been investigated by simulating the steps of the postulated catalytic cycle (Fig. 8a).¹⁰¹

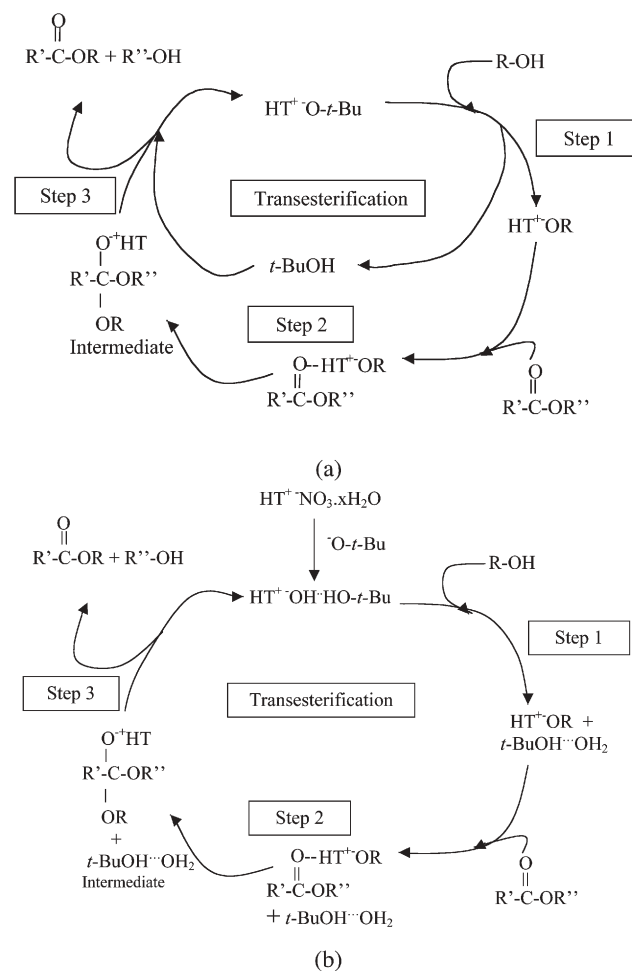


Fig. 8 Scheme to show (a) the mechanism proposed by Choudary *et al.* for the catalytic process, after experimental work by Choudary *et al.*³³ and (b) the reaction mechanism for the *trans*-esterification reaction, as suggested by the simulations outlined in this Section. The catalyst used is, in fact, a hydroxide-intercalated MgAl LDH generated by deprotonation of interlayer water by the *t*-butoxide. The organophilic interlayer environment resulting from the *t*-butyl groups of associated *t*-butanol molecules enhances the catalytic properties. Catalyst regeneration can now occur, which was not observed in the scheme proposed by Choudary *et al.* In the diagram R denotes CH_3 or C_2H_5 ; R' is a normal or β -ketoester; R'' may be a primary, secondary, unsaturated, allylic, cyclic, hindered alcohol or amine.

This work was undertaken using the CASTEP code.¹⁰² The size of model necessary to incorporate all the participating species, under fully solvated conditions, would be too large to allow electronic structure simulation over chemically meaningful time scales. The absence of interlayer solvent would result in the model system interlayer collapsing relative to the experimental system, so a fixed interlayer spacing is advantageous rather than a handicap for the modeller. Due to the extremely high computational cost of such studies, a simple interlayer environment was created, with just one Al atom per unit cell and an initial interlayer spacing of 16 Å. The transesterification of methylacetoacetate with prop-2-en-1-ol was selected as a representative system to simulate.¹⁰¹

Interactions between the LDH host and the organic substrate molecules were investigated for each step of the experimentally postulated mechanism; this was found not to allow catalyst regeneration in the simulation work, and an alternative mechanism was proposed that is consistent with both experiment and simulation, as given in Fig. 7b. Catalyst regeneration only occurred when interlayer water molecules were present, a scenario shown in the simulations to be inconsistent with the presence of *tert*-butoxide anions in the interlayer. The modelling established that the active catalyst was, in fact, a hydroxide intercalated LDH, with neutral *t*-butanol molecules associated with the LDH layer. A reduced interlayer spacing of 10.50 Å was also required for the catalyst to regenerate. The regeneration step is illustrated in Fig. 9.

Experimental evidence for the high activity of the hydroxide MgAl LDH lends support to these findings,¹³ as does another study into the electronic structure of hydroxide intercalated LDHs by Trave *et al.*¹⁰³ The study of the *trans*-esterification reaction illustrates the importance of the H-bonding environment within the LDHs. The combination of the variable interlayer spacing of the LDHs, which allows more specificity to substrate molecules, and the amphiphilic nature of the galleries, caused by a hydrophilic layer adjacent to the LDH layer and an organophilic region in the interlayer centre (due to the *t*-butyl groups), is deemed to be responsible for the increased catalytic activity of these materials.⁹⁶ Thus organic substrate molecules are more easily adsorbed within the organophilic interlayer region with their polar reactive groups oriented by the LDH layer surface, greatly facilitating subsequent chemical reactions when compared to the organophobic rehydrated hydroxide LDH.⁹⁶

6.2. Acid catalysis by cationic clays during *in situ* polymerisation reactions for the formation of clay–polymer nanocomposites

Interest in the catalytic properties of clay minerals has also arisen out of a desire to better understand and control new synthetic routes to clay–polymer nanocomposites. Experimental work by Coveney *et al.* indicated that when the natural and unmodified clay mineral montmorillonite is treated with a solution of methanal and ethylenediamine under mild conditions, the monomers spontaneously copolymerise to form an intercalated clay–polymer nanocomposite material with desirable properties,^{74,75} although it was unclear how the clay mineral might be acting as a catalyst for the reaction. As

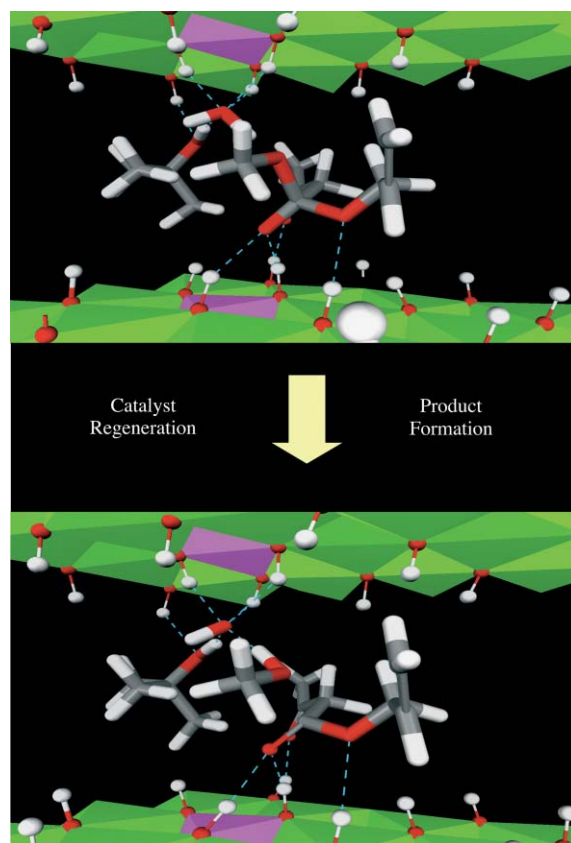


Fig. 9 Snapshot of MD simulation showing catalyst regeneration: (a) model after 159 fs simulation showing rearrangement of intermediate, and (b) model after 269 fs of simulation showing regeneration of basic catalyst site.

mentioned previously, both Lewis acidity and Brønsted acidity are possible in cationic clay minerals.

In this context Stackhouse *et al.* performed density functional calculations on a periodic montmorillonite model to investigate the catalytic role played by the clay mineral in the reaction.¹⁰⁴ A variety of possible Brønsted and Lewis acid sites were investigated to understand their role in increasing the susceptibility of the methanal C=O carbonyl towards nucleophilic attack. Initial simulations indicated that methanal could only undergo nucleophilic attack by ethylenediamine when suitably activated either by protonation or coordination to a suitable Lewis acid.

These original studies considered only the interlayer species of the natural clay, various cations and water molecules, and showed that the interlayer cation, when modelled *in vacuo* with the two organic species, could feasibly be sufficiently activating to promote the reaction.¹⁰⁴ However, further consideration of the interlayer conditions, where the cations are likely to be screened from the methanal by water molecules, suggested that this approach may not represent the full story. Using similar simplistic models, the relative ability of various cations to deprotonate interlayer water was considered. It was found that only Mg²⁺ and Al³⁺ were sufficiently polarising to induce deprotonation of the water molecule by methanal, the polarising ability of the cations tested being: Al³⁺ > Mg²⁺ > Ca²⁺ > Na⁺. Once again, as the deprotonation of water

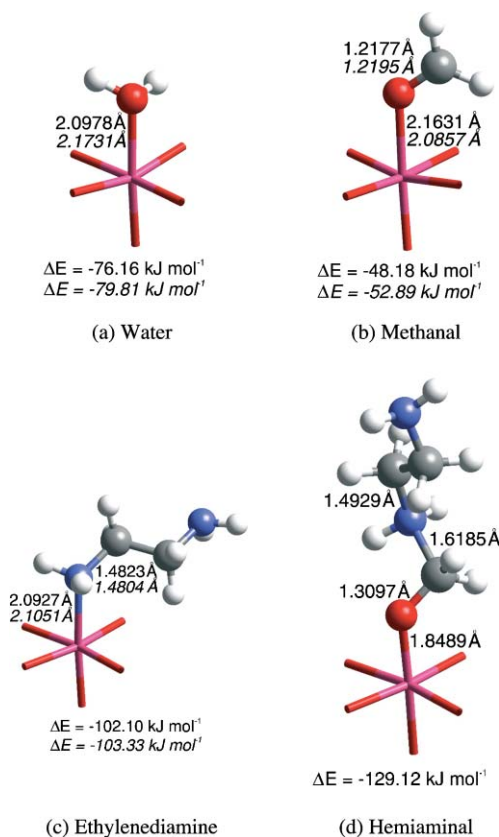


Fig. 10 Optimised geometry of species co-ordinated to an exposed aluminium atom in the octahedral layer of a montmorillonite cationic clay lattice-edge. Bond lengths and adsorption energies for each model are presented, with analogous values for the pyrophyllite lattice-edge model given in italics.

occurred only when Mg^{2+} and Al^{3+} were used rather than the more common naturally occurring interlayer cations Na^+ and Ca^{2+} , it was considered that the interlayer cation played little part in catalysing the polymerization reaction.

Having noted that the interlayer cations and water may have a limited role in clay catalysis, the effect of the structure of the clay sheet was considered. Stackhouse *et al.* subsequently investigated the effects of isomorphous substitution (Al^{3+} by Mg^{2+} or Si^{4+} by Al^{3+}) upon Brønsted acidity of hydroxyl groups located in the octahedral layer, the tetrahedral layer and at edge sites. Protonation of the methanal molecule was not observed in any of these scenarios, suggesting that the initial step in the *in situ* polymerization reaction was unlikely to be Brønsted acid catalysed. The Lewis acidity of exposed Al atoms at edge sites on the clay sheets was therefore considered. Fig. 10 and Fig. 11 show the effect of lattice-edge sites on polarising the reactive species at octahedral and tetrahedral sites, respectively. These were shown to exhibit a catalytic effect, the magnitude of which was found to be strongly dependent upon the degree of substitution of Al^{3+} by Mg^{2+} in the octahedral layer of the clay sheets.¹⁰⁴

In summary, the electronic structure investigation of *in situ* polymerisation suggests that copolymerisation may be initially catalysed by exposed aluminium ions acting as Lewis acid sites, and located at the clay mineral lattice-edge. The subsequent

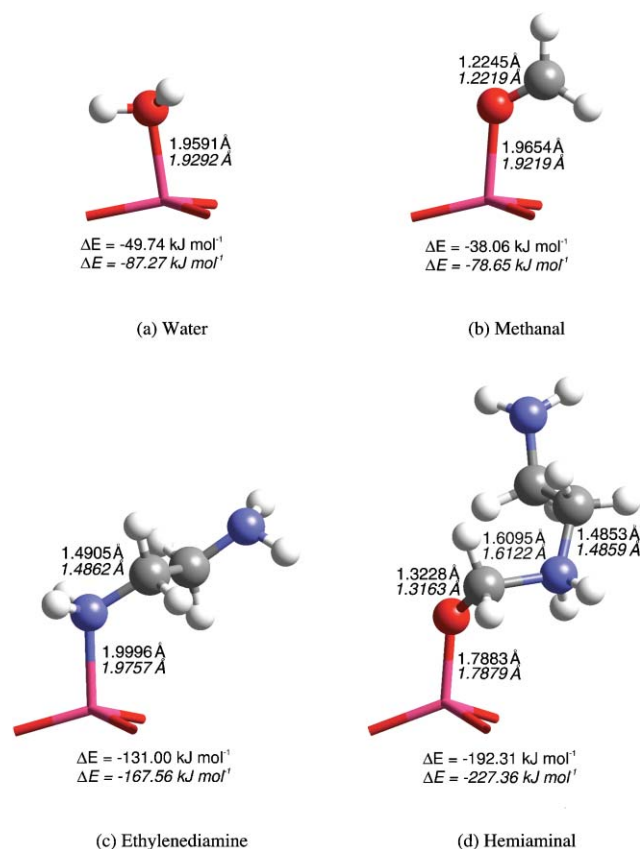


Fig. 11 Optimised geometry of species co-ordinated to an exposed aluminium atom in the tetrahedral layer of a montmorillonite cationic clay lattice-edge. Bond lengths and adsorption energies for each model are presented, with analogous values for the pyrophyllite lattice-edge model given in italics.

reactions are probably catalysed by a mixture of Lewis and Brønsted acidity, which needs future investigation.

7. The future of computer simulation in materials chemistry

Over recent years, it has been shown that computer simulation provides considerable insight into the interlayer properties and dynamics of many clay-based materials, often in a very applied and relevant fashion. As computational algorithms and hardware have developed so too has the size and detail of the systems simulated.

We have seen that, in the past, the simulation of chemical reactions in clay interlayers, or at clay surfaces is computationally expensive, and in cases such as photochemical reactions where excited states need to be considered the computational chemist has been restricted. However, recent work in the development of time dependent DFT (TDDFT) techniques, yet to be applied to clays, shows potential for addressing these difficult areas; TDDFT has been reviewed recently by Oneda *et al.*¹⁰⁵ Other work has been addressed at gaining accurate binding energies of cations at clay surfaces using the technique of thermodynamic integration (TI) coupled with DFT calculations.¹⁰⁶ Recently, there has been increased interest in modelling inorganic crystal growth

processes, and Sato *et al.* have investigated growth processes in brucite (Mg(OH)₂), which is closely related to the anionic clay family of materials, using electronic structure methods.¹⁰⁷

From a methodological perspective, the use of periodic boundary conditions to enable the calculation of bulk structure and properties has become the norm for both electronic structure and force-field based simulations in materials science and offers an efficient way to simulate bulk material and interfaces. However, as classical MD simulations begin to reach the scale of millions of atoms, the periodic conditions become unnecessarily restrictive, resulting in artificial constraints and preventing the simulation of intercalation processes. Indeed, it will soon be possible to simulate entire clay platelets and finite size effects will be eliminated in very large molecular dynamics models.

Increasingly, the simulation of long time-scales and/or large models lies within the computational resources available to the computational materials chemist. Further limitations may be circumvented in the future through the use of Grid computing where simulations are not just run on single high performance computers, but instead harness large numbers of super-computers distributed around the globe.¹⁰⁸

A major goal in computational science is to be able to simulate a given system over an extensive range of length and time-scales from the electronic structure through to the continuum level, using information from one level of modelling to increase the accuracy, or extend the time-scale, of another.^{109–111} Already electronic structure techniques, force-field based molecular dynamics and mesoscopic dynamics are allowing chemists and materials scientists to explore clay structure, properties and dynamical behaviour not readily accessible by experimental means of characterisation. Computable quantities that may be directly compared to experimental values such as interlayer separations, chemical reactivity, and diffusion coefficients are today readily obtained. The outstanding challenge for the future is to integrate these techniques to provide a more complete multi-scale understanding of these ubiquitous and important materials.^{112,113}

Acknowledgements

The authors are grateful to Accelrys Inc. for provision of various software packages used throughout this work. Both HCG and PVC thank the EPSRC (GR/R30907 and GR/R67699); HCG also thanks the Isaac Newton Trust, Cambridge for funding during this period. SS acknowledges NERC, W. R. Grace & Co., Conn., and Queen Mary University of London for funding.

References

- 1 R. A. Schoonheydt, T. J. Pinnavaia, G. Lagaly and N. Gangas, *Pure Appl. Chem.*, 1999, **71**, 2367–2371.
- 2 R. E. Grim, *Applied Clay Mineralogy*, 1962, McGraw-Hill Book Company, New York.
- 3 S. P. Newman and W. Jones, *New J. Chem.*, 1998, **22**, 105–115.
- 4 F. Cavani, F. Trifirò and A. Vaccari, *Catal. Today*, 1991, **11**, 173–301.
- 5 S. Carlino, *Chem. Br.*, 1997, **33**, 59–62.
- 6 G. Lagaly and K. Beneke, *Colloid Polym. Sci.*, 1991, **269**, 1198–1211.
- 7 S. P. Newman, S. J. Williams, P. V. Coveney and W. Jones, *J. Phys. Chem. B*, 1998, **102**, 6710–6719.
- 8 J. Swenson, G. A. Schwartz, R. Bergman and W. S. Howells, *Eur. Phys. J. E*, 2003, **12**, 179–183.
- 9 W. W. Kagunya, *J. Phys. Chem.*, 1996, **100**, 327–330.
- 10 *Layered Double Hydroxides: Present and Future*, ed. V. Rives, Nova Science, New York, 2001.
- 11 R. W. McCabe, Clay Chemistry, in *Inorganic Materials*, D. W. Bruce and D. O'Hare, Wiley, New York, 1992, pp 295–351.
- 12 W. T. Reichle, *J. Catal.*, 1985, **94**, 547–557.
- 13 V. R. L. Constantino and T. J. Pinnavaia, *Inorg. Chem.*, 1995, **34**, 883–892.
- 14 K. K. Rao, M. Gravelle, J. S. Valente and F. Figueras, *J. Catal.*, 1998, **173**, 115–121.
- 15 B. M. Choudary, M. L. Kantam, B. Bharathi and C. V. Reddy, *SYNLETT*, 1998, 1203–1204.
- 16 J. Tronto, E. L. Crepaldi, P. C. Pavan, C. C. De Paula and J. B. Valim, *Mol. Cryst. Liq. Cryst.*, 2001, **356**, 227–237.
- 17 J. H. Choy, S. Y. Kwak, Y. J. Jeong and J. S. Park, *Angew. Chem., Int. Ed.*, 2000, **39**, 4042–4045.
- 18 J.-H. Choy, J.-M. Oh, M. Park, K.-M. Sohn and J.-W. Kim, *Adv. Mater.*, 2004, **16**, 1181–1184.
- 19 Y. H. Guo, D. F. Li, C. W. Hu, Y. H. Wang, E. B. Wang, Y. C. Zhou and S. H. Feng, *Appl. Catal., B*, 2001, **30**, 337–349.
- 20 A. Meunier, B. Velde and L. Griffault, *Clay Miner.*, 1998, **33**, 187.
- 21 *Polymer-Clay Nanocomposite*, T.J. Pinnavaia and G.W. Beall, Chichester, John Wiley & Sons Ltd, 2000.
- 22 F. Figueras, *Top. Catal.*, 2004, **29**, 189–196.
- 23 S. R. Chitnis and M. M. Sharma, *React. Funct. Polym.*, 1997, **32**, 93–115.
- 24 B. Sels, D. De Vos, M. Buntinx, F. Pierard, A. Kirsch-De Mesmaeker and P. Jacobs, *Nature*, 1999, **400**, 855–857.
- 25 T.-Q. Li, M. Häggkvist and L. Ödberg, *Colloids Surf., A*, 1999, **159**, 57.
- 26 G. Onkal-Engin, R. Wibulswas and D. A. White, *Environ. Technol.*, 2000, **21**, 167–175.
- 27 S. Cheng, *Catal. Today*, 1999, **49**, 303–312.
- 28 (a) A. R. Leach, *Molecular Modelling, Principles and Applications*, Pearson Education Ltd, England, 2nd edn., 2001; (b) M. P. Allen and D. J. Tildesley, *Computer Simulation of Liquids*, Clarendon, Oxford, 1987; (c) D. Frenkel and B. Smit, *Understanding Molecular Simulation: From Algorithms to Applications*, Academic Press, London, England, 2nd edn., 2002.
- 29 B. A. Luty, M. E. Davis, I. G. Tironi and W. F. Vangunsteren, *Mol. Simul.*, 1994, **14**, 11–20; A. Y. Toukmaji and J. A. Board, *Comput. Phys. Commun.*, 1996, **95**, 73–92.
- 30 M. Tuckerman, B. J. Berne and G. J. Martyna, *J. Chem. Phys.*, 1992, **97**, 1990–2001.
- 31 B. J. Teppen, K. Rasmussen, P. M. Bertsch, D. M. Miller and L. Schäfer, *J. Phys. Chem. B*, 1997, **101**, 1579–1587.
- 32 R. T. Cygan, J. J. Liang and A. G. Kalinichev, *J. Phys. Chem. B*, 2004, **108**, 1255–1266.
- 33 S. P. Newman, H. C. Greenwell, P. V. Coveney and W. Jones, Computer modelling of layered double hydroxides, in *Layered Double Hydroxides: Present and Future*, ed. V. Rives, Nova Science, New York, 2001.
- 34 D. Spangberg and K. Hermansson, *J. Chem. Phys.*, 2004, **120**, 4829–4843.
- 35 M. J. Elrod and R. J. Saykally, *Chem. Rev.*, 1994, **94**, 1975–1997.
- 36 T. P. Lybrand and P. A. Kollman, *J. Chem. Phys.*, 1985, **83**, 2923–2933.
- 37 A. G. Kalinichev, R. J. Kirkpatrick and R. T. Cygan, *Am. Mineral.*, 2000, **85**, 1046–1052.
- 38 J. W. Wang, A. G. Kalinichev, R. J. Kirkpatrick and X. Q. Hou, *Chem. Mater.*, 2001, **13**, 145–150.
- 39 X. Q. Hou, A. G. Kalinichev and R. J. Kirkpatrick, *Chem. Mater.*, 2002, **14**, 3539–3549.
- 40 X. Q. Hou, D. L. Bish, S. L. Wang, C. T. Johnston and R. J. Kirkpatrick, *Am. Mineral.*, 2003, **88**, 167–179.
- 41 J. W. Wang, A. G. Kalinichev, J. E. Amonette and R. J. Kirkpatrick, *Am. Mineral.*, 2003, **88**, 398–409.
- 42 J. O. Titiloye and N. T. Skipper, *Chem. Phys. Lett.*, 2000, **329**, 23–28.

- 43 G. Sposito, N. T. Skipper, R. Sutton, S. H. Park, A. K. Soper and J. A. Greathouse, *Proc. Natl. Acad. Sci. USA*, 1999, **96**, 3358–3364.
- 44 E. S. Boek, P. V. Coveney and N. T. Skipper, *J. Am. Chem. Soc.*, 1995, **117**, 12608–12617.
- 45 H. Sato, A. Yamagishi and K. Kato, *J. Am. Chem. Soc.*, 1992, **114**, 10933–10940.
- 46 H. Sato, A. Yamagishi and K. Kato, *J. Phys. Chem.*, 1992, **96**, 9377–9382.
- 47 H. Sato, A. Yamagishi and K. Kato, *J. Phys. Chem.*, 1992, **96**, 9382–9387.
- 48 O. L. Manevitch and G. C. Rutledge, *J. Phys. Chem. B*, 2004, **108**, 1428–1435.
- 49 H. Sato, A. Yamagishi and K. Kawamura, *J. Phys. Chem. B*, 2001, **105**, 7990–7997.
- 50 M. A. Drezdon, *Inorg. Chem.*, 1988, **27**, 4628–4632.
- 51 F. Kooli, I. C. Chisem, M. Vucelic and W. Jones, *Chem. Mater.*, 1996, **8**, 1969–1977.
- 52 J. King and W. Jones, *Mol. Cryst. Liq. Cryst.*, 1992, **211**, 257–270.
- 53 A. M. Aicken, I. S. Bell, P. V. Coveney and W. Jones, *Adv. Mater.*, 1997, **9**, 496–501.
- 54 E. S. Boek, P. V. Coveney, S. J. Williams and A. S. Bains, *Mol. Simul.*, 1996, **18**, 145–154.
- 55 R. Mills, *J. Phys. Chem.*, 1973, **77**, 685.
- 56 S. J. Williams, P. V. Coveney and W. Jones, *Mol. Simul.*, 1999, **21**, 183–189.
- 57 T. Hibino and M. Kobayashi, *J. Mater. Chem.*, 2005, **15**, 653–656.
- 58 A. S. Bains, E. S. Boek, P. V. Coveney, S. J. Williams and M. V. Akbar, *Mol. Simul.*, 2001, **26**, 101.
- 59 M. Ogawa and K. Kuroda, *Chem. Rev.*, 1995, **95**, 399–438.
- 60 J. Valim, B. M. Kariuki, J. King and W. Jones, *Mol. Cryst. Liq. Cryst.*, 1992, **211**, 271.
- 61 K. Takagi, T. Shichi, H. Usami and Y. Sawaki, *J. Am. Chem. Soc.*, 1993, **115**, 4339.
- 62 T. Shichi, K. Takagi and Y. Sawaki, *Chem. Commun.*, 1996, 2027.
- 63 S. P. Newman, H. C. Greenwell, P. V. Coveney and W. Jones, *J. Mol. Struct.*, 2003, **647**, 1–3, 75.
- 64 F. Leroux, P. Aranda, J. P. Besse and E. Ruiz-Hitzky, *Eur. J. Inorg. Chem.*, 2003, **6**, 1242–1251.
- 65 B. Chen, *Br. Ceram. Trans.*, 2004, **6**, 103.
- 66 J. Bujdák, E. Hackett and E. P. Giannelis, *Chem. Mater.*, 2000, **12**, 2168–2174.
- 67 R. Toth, A. Coslanich, M. Ferrone, M. Fermeglia, S. Pricl, S. Miertus and E. Chiellini, *Polymer*, 2004, **45**, 8075–8083.
- 68 M. Fermeglia, M. Ferrone and S. Pricl, *Mol. Simul.*, 2004, **30**, 289–300.
- 69 M. Fermeglia, M. Ferrone and S. Pricl, *Fluid Phase Equilib.*, 2003, **212**, 315–329.
- 70 T. Lan, P. Kaviratna and T. J. Pinnavaia, *J. Phys. Chem. Solids*, 1996, **57**, 1005–1010.
- 71 J.-J. Lin and Y.-M. Chen, *Langmuir*, 2004, **20**, 4261–4264.
- 72 P. Boulet, A. A. Bowden, P. V. Coveney and A. Whiting, *J. Mater. Chem.*, 2003, **13**, 2540–2550.
- 73 H. C. Greenwell, M. J. Harvey, P. Boulet, A. A. Bowden, P. V. Coveney and A. Whiting, *Macromolecules*, 2005, **38**, 14, 6189–6200.
- 74 P. V. Coveney, M. Watkinson, A. Whiting and E. S. Boek, *Stabilizing Clayey Formations*, US Patent Number 6 787 507, 2004.
- 75 P. V. Coveney, J. L. W. Griffin, M. Watkinson, A. Whiting and E. S. Boek, *Mol. Simul.*, 2002, **28**, 295.
- 76 H. C. Greenwell, A. A. Bowden, P. Boulet, B. Q. Chen, J. R. G. Evans, P. V. Coveney and A. Whiting, *J. Mater. Chem.*, 2005, DOI: 10.1039/b505217c, in review.
- 77 J. Hein, F. Reid, L. Smith, I. Bush, M. Guest and P. Sherwood, *Philos. Trans. R. Soc. London, Ser. A*, 2005, **363**, 1987–1999.
- 78 D. R. Katti, S. R. Schmidt, P. Ghosh and K. S. Katti, *Clays Clay Miner.*, 2005, **53**, 171–178.
- 79 S. Plimpton, *J. Comput. Phys.*, 1995, **117**, 1–19.
- 80 P. V. Coveney and H. C. Greenwell, *Geochim. Cosmochim. Acta*, 2004, **68**, 11, A106 Suppl.
- 81 E. Lindahl and O. Edholm, *Biophys. J.*, 2000, **79**, 426–433.
- 82 H. Sato, A. Yamagishi and K. Kawamura, *J. Phys. Chem. B*, 2001, **105**, 7990–7997.
- 83 A. Sinsawat, K. L. Anderson, R. A. Vaia and B. L. Farmer, *J. Polym. Sci., Part B: Polym. Phys.*, 2003, **41**, 3272–3284.
- 84 B. J. Teppen, C.-H. Yu, S. Q. Newton, D. M. Miller and L. Schäffer, *J. Mol. Struct.*, 1998, **445**, 65.
- 85 D. Bougeard, K. S. Smirnov and E. Geidel, *J. Phys. Chem. B*, 2000, **104**, 9210.
- 86 C. I. Sianz-Diaz, V. Timon, V. Botella and A. Hernandez-Laguna, *Am. Mineral.*, 2000, **85**, 1038.
- 87 B. J. Teppen, C.-H. Yu, S. Q. Newton, D. M. Miller and L. Schäffer, *J. Phys. Chem. A*, 2002, **106**, 5498.
- 88 L. Benco, D. Tunega, J. Hafner and H. Lishka, *Am. Mineral.*, 2001, **86**, 1057.
- 89 C. H. Bridgeman, A. D. Buckingham, N. T. Skipper and M. C. Payne, *Mol. Phys.*, 1996, **89**, 879.
- 90 S. Stackhouse and P. V. Coveney, *J. Phys. Chem. B*, 2002, **106**, 12470–12477.
- 91 S. Stackhouse, P. V. Coveney and D. M. Benoit, *J. Phys. Chem. B*, 2004, **108**, 9685–9694.
- 92 G. L. Gorb, J. Gu, D. Leszczynska and J. Leszczynski, *Phys. Chem. Chem. Phys.*, 2000, **2**, 5007.
- 93 D. Tunega, L. Benco, G. Haberhauer, M. H. Gerzabeck and H. Lischka, *J. Phys. Chem. B*, 2002, **106**, 11515.
- 94 A. Chatterjee, T. Iwasaki and T. Ebina, *J. Phys. Chem. A*, 2000, **104**, 8216.
- 95 E. S. Boek and M. Sprik, *J. Phys. Chem. B*, 2003, **107**, 3251.
- 96 H. C. Greenwell, S. Stackhouse, P. V. Coveney and W. Jones, *J. Phys. Chem. B*, 2003, **107**, 3476.
- 97 B. M. Choudary, M. L. Kantam, B. Bharathi and C. V. Reddy, *SYNLETT*, 1998, 1203–1204.
- 98 B. M. Choudary, M. L. Kantam, B. Kavita, C. V. Reddy, K. K. Rao and F. Figueras, *Tetrahedron Lett.*, 1998, **39**, 3555–3558.
- 99 B. M. Choudary, M. L. Kantam and B. Kavita, *Green Chem.*, 1999, **1**, 289–292.
- 100 B. M. Choudary, M. L. Kantam, B. Kavita, C. V. Reddy and F. Figueras, *Tetrahedron*, 2000, **56**, 9357–9364.
- 101 B. M. Choudary, M. L. Kantam, C. V. Reddy, S. Aranganathan, P. L. Santhi and F. Figueras, *J. Mol. Catal. A: Chem.*, 2000, **159**, 411–416.
- 102 M. D. Segall, P. J. D. Lindan, M. J. Probert, C. J. Pickard, P. J. Hasnip, S. J. Clark and M. C. Payne, *J. Phys.: Condens. Matter*, 2002, **14**, 2717–2744.
- 103 A. Trave, A. Selloni, A. Goursot, D. Tichit and J. Weber, *J. Phys. Chem. B*, 2002, **106**, 12291–12296.
- 104 S. Stackhouse, P. V. Coveney and E. Sandré, *J. Am. Chem. Soc.*, 2001, **123**, 11764.
- 105 G. Onida, L. Reining and A. Rubio, *Rev. Mod. Phys.*, 2002, **74**, 601–659.
- 106 J. L. Suter, *Ab initio Molecular Dynamics Investigation of 2 : 1 Smectite Clay Systems and Atomic Charges*, PhD Thesis, University of Cambridge, Cambridge, 2005.
- 107 H. Sato, A. Morita, K. Ono, H. Nakano, N. Wakabayashi and A. Yamagishi, *Langmuir*, 2003, **19**, 7120–7126.
- 108 *Phil. Trans. R. Soc. A.*, 2005, **363**, 1701–2095, ed. P. V. Coveney.
- 109 N. Sheng, M. C. Boyce, D. M. Parks, G. C. Rutledge, J. I. Abes and R. E. Cohen, *Polymer*, 2004, **45**, 487–506.
- 110 Y. Ichikawa, K. Kawamura, N. Theramast and K. Kitayama, *Mech. Mater.*, 2004, **36**, 487–513.
- 111 P. Porion, M. Al Mukhtar, A. M. Faugère, R. J. M. Pellenq, S. Meyer and A. Delville, *J. Phys. Chem. B*, 2003, **107**, 4012–4023.
- 112 R. M. Nieminen, *J. Phys.: Condens. Matter*, 2002, **14**, 2859–2876.
- 113 P. V. Coveney and P. W. Fowler, *J. R. Soc. London: Interface*, 2005, **363**, 267–280.